Genes & Diseases (2023) 10, 10–13

Available online at www.sciencedirect.com

ScienceDirect

journal homepage: www.keaipublishing.com/en/journals/genes-diseases

RAPID COMMUNICATION

Nuclear lncRNA CERNA1 enhances the cisplatin-induced cell apoptosis and overcomes chemoresistance via epigenetic activation of BCL2L10 in ovarian cancer

Ovarian cancer (OC) is the most lethal type of cancer among female genital tumors.[1] Along with debulking surgeries, platinum is the first-line chemotherapy treatment, whereas chemoresistance is the biggest obstacles in a poor prognosis of OC.[2] Identifying a novel therapeutic target for OC chemoresistance remains an urgent need. lncRNAs are expressed in tissue-specific patterns and distributed in the specific subcellular locations. The diverse regulatory mechanisms of lncRNAs are dependent on their subcellular location.[3,4] lncRNA CERNA1, which is mainly located in the cytoplasm of HUVECs, acts as a miRNA sponge.[5] Here, for the first time, we described the role and the molecular regulatory mechanism of nuclear CERNA1 in OC. We found that CERNA1 was poorly expressed in both OC tissues and OC cells, which predicts a poor OC prognosis. Unlike in HUVECs, CERNA1 is distributed almost exclusively in the nucleus of OC cells. Nuclear CERNA1 induced BCL2L10 expression (an OC tumor repressor), promoted cell apoptosis and reduced the cisplatin resistance by decoying DNMT1 from the BCL2L10 promoter. These results suggest that CERNA1 might be an attractive therapeutic target for improving the sensitivity to chemotherapy for OC patients.

Long noncoding RNAs (lncRNAs) constitute a large portion of the mammalian transcriptome. A set of the OC-related lncRNAs that act as oncogenes or tumor suppressors has been previously reported, including HOTAIR, lncRNA ATB, lncRNA E2F4as and lncRNA SNHG17. lncRNA CERNA1 (competing endogenous lncRNA 1 for miR-4707-5p and miR-4767), formerly known as LOC100129973, was first identified in ABO (6-amino- 2,3-dihydro-3-hydroxymethyl-1,4-benzoxazine) to relieve the serum and FGF-2 starvation-induced apoptosis of human umbilical vein endothelial cells (HUVECs). With the decoy activity of sequestering miR-4707-5p and miR-4767, CERNA1 promotes the expression of API5 and BCL2L12, and thus suppresses apoptosis. However, there are no reports about CERNA1 in any tumor. To explore the function of CERNA1 in OC, we analyzed the data of OC tissues in GEO profiles and identified that CERNA1 expression was significantly downregulated in OC tissues (Fig. S1A, B) and its expression further decreased with the development of platinum resistance (Fig. S1C, D). We determined the CERNA1 expression in 18 pairs of ovarian tumors and adjacent non-tumor tissues. Consistent with the microarray results, CERNA1 expression in tumor tissues was significantly decreased (Fig. S1E). Furthermore, the results from GEPIA datasets showed that CERNA1 was downregulated in OC samples and that CERNA1 expression declined continuously along with the OC progression (Fig. S1F, G). Moreover, the survival analysis results demonstrated that OC patients with low CERNA1 expression had a significantly worse prognosis (Fig. S1H). These results showed that CERNA1 expression was extremely low in OC and that the down-regulated expression predicts poor outcomes in OC patients.

CERNA1 expression in OC cells was lower than in normal human ovarian surface epithelial cells (HOSE) (Fig. S2A). SKOV3 was selected to create an overexpression and knockdown cell model due to its moderate CERNA1 expression. Considering that CERNA1 expression was associated with platinum resistance, we hypothesized that CERNA1 was involved in the cisplatin-induced OC cell apoptosis. qRT-PCR analysis showed that CERNA1 expression was upregulated by cisplatin treatment (Fig. 1A). Furthermore, we detected the subcellular distribution of CERNA1 in OC cells. The results showed that the majority of CERNA1 was distributed in the nuclei of OC cells (Fig. 1B). SnoVector — a construct generated for stable nuclear

Peer review under responsibility of Chongqing Medical University.

https://doi.org/10.1016/j.gendis.2021.12.018

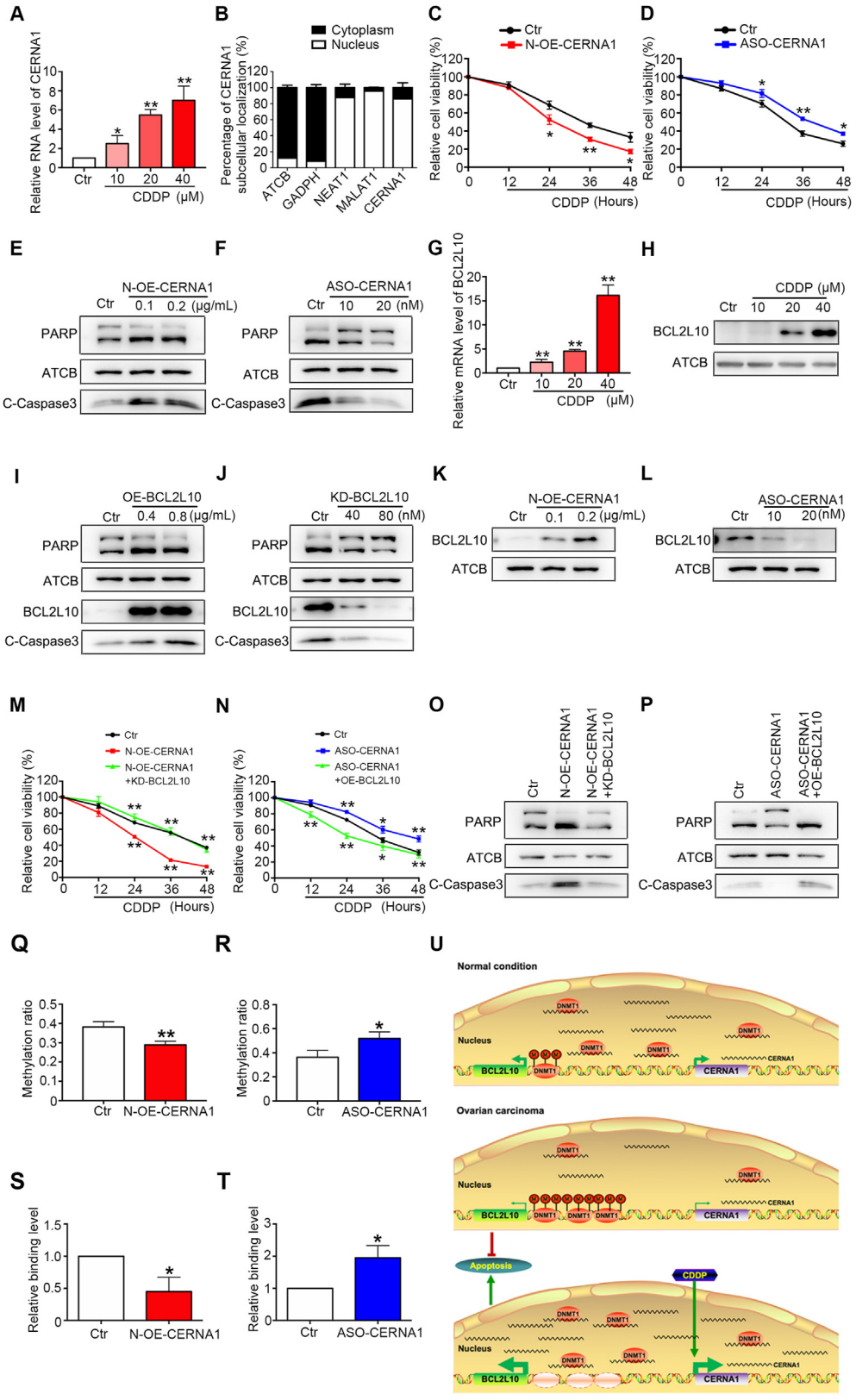

Figure 1 Nuclear CERNA1 enhanced BCL2L10 expression by decoying DNMT1 from BCL2L10 promoter, thus promoted the cisplatin induced cell apoptosis in ovarian cancer. **(A)** Quantified real-time PCR analysis of CERNA1 expression treated with cisplatin for 24 h at various concentration in SKOV3 cells. **(B)** The cellular distribution of CERNA1 in SKOV3 cells. Cells were separated into two fractions and then RNA was separately extracted from nucleus and cytoplasm; qPCR was used to detect CERNA1 RNA level (ATCB and GAPDH as cytoplasmic marker; MALAT1 and NEAT1 as nuclear marker). **(C, D)** CCK8 analysis of SKOV3 cell viability. SKOV3 cells

lncRNA expression — was used to overexpress CERNA1 in the nuclei of cells (N-OE-CERNA1). For knocking down nuclear lncRNA, ASOs were used to silence CERNA1 expression (Fig. S2B, C). N-OE-CERNA1, ASO-CERNA1 and their controls were transfected into SKOV3 cells with cisplatin treatment at different time points. The CCK8 assay indicated that OC cells with nuclear CERNA1 overexpression exhibited higher sensitivity to platinum cytotoxicity, whereas, nuclear CERNA1 knockdown conferred OC cells with platinum resistance (Fig. 1C, D). Moreover, nuclear CERNA1 significantly elevated the level of cleaved PARP and cleaved Caspase 3; correspondingly, nuclear CERNA1 knockdown significantly inhibited the PARP and Caspase 3 cleavage (Fig. 1E, F; Fig. S2D—G). Taken together, CERNA1, mainly located in the nucleus of OC cells, enhanced the cisplatin induced apoptosis, thus reducing the cisplatin resistance.

BCL2L10 is located in chromosome 15, the neighboring region of CERNA1 in the genome (Fig. S3A). To explore the expression pattern of BCL2L10 in OC, the data from the GEO profile (GDS3592) were analyzed. The results demonstrated that the BCL2L10 mRNA level was significantly lower in OC tissues (Fig. S3B, C). Furthermore, tissues were graded into either the high-expression or low-expression groups, according to the immunohistochemical staining of BCL2L10. Low expression of BCL2L10 was found in 75% of the OC samples ($n = 52$), whereas it only accounted for 33% in adjacent non-tumor tissue ($n = 32$) (Fig. S3D, E). We analyzed the correlation between BCL2L10 expression and FIGO stage with the TCGA database. Results showed that, the expression of BCL2L10 was significantly decreased and accompanied by the OC progression (Fig. S3F). A Kaplan—Meier survival analysis proved that OC patients with high BCL2L10 levels had longer survival than OC patients with low BCL2L10 (Fig. S3G). Moreover, a positive correlation was noted between CERNA1 and BCL2L10 in their expression, with a correlation coefficient of 0.42 (Fig. S3H). These data suggest that a low level of BCL2L10 existed in OC tissues; a lower expression predicted a worse prognosis.

Considering the role of CERNA1 in cisplatin resistance of OC, we wondered whether BCL2L10 was involved in cisplatin-induced apoptosis. Both the mRNA and protein levels of BCL2L10 were dramatically increased under cisplatin treatment (Fig. 1G, H; Fig. S4A). The pcDNA3.1-BCL2L10 plasmid was transfected into SKOV3 for BCL2L10 overexpression (OE-BCL2L10). Both siBCL210 and ASO-BCL2L10 were simultaneously transfected into SKOV3 for BCL2L10 knockdown (KD-BCL2L10). The efficiency of overexpression or knockdown was determined by Western blot analysis. BCL2L10 overexpression efficiently increased the level of cleaved PAPR and cleaved Caspase 3. For the knockdown of BCL2L10, the cleaved PARP and Caspase 3 were evidently inhibited (Fig. 1I, J; Fig. S4B—G). Collectively, BCL2L10 acted as a tumor repressor and promoted the cisplatin-induced apoptosis.

Next, we evaluated the mRNA and protein levels of BCL2L10 after overexpression or knockdown of nuclear CERNA1. When nuclear CERNA expression was enhanced, BCL2L10 expression was significantly increased. In contrast, BCL2L10 expression decreased (Fig. 1K, L; Fig. S5A—D). The CCK8 assay suggested that the cisplatin resistance reduced by nuclear CERNA1 overexpression was recovered after BCL2L10 knockdown. Conversely, the cisplatin resistance enhanced by nuclear CERNA1 knockdown was restored after BCL2L10 overexpression (Fig. 1M, N). Furthermore, BCL2L10 knockdown significantly inhibited the cleavage of PARP and Caspase 3, which was induced by N-OE-CERNA1. Correspondingly, overexpression of BCL2L10 significantly promoted the cleavage of PARP and Caspase 3, which was inhibited by ASO-CERNA1 (Fig. 1O, P; Fig. S5E—H). Collectively, nuclear CERNA1 promoted the cisplatin-induced

were transfected with pZW1-sno-CERNA1 and empty vector at 0.2 μg/mL for 24 h (C), or ASO-CERNA1 and ASO-negative control at 20 nM (D), and then treated with 20 μM cisplatin for another 12, 24, 36 and 48 h. **(E, F)** Western blot analysis of cleaved PARP, ATCB and cleaved Caspase 3 protein levels. SKOV3 cells were transfected with pZW1-sno-CERNA1 (E) or ASO-CERNA1 (F) for 24 h and then treated with 20 μM cisplatin for another 24 h (E) or 36 h (F). **(G, H)** Quantified real-time PCR analysis of BCL2L10 mRNA level (G) and Western blot analysis of BCL2L10 protein level (H) after treated with cisplatin for 24 h at various concentration in SKOV3 cells. **(I, J)** Western blot analysis of cleaved PARP, ATCB, BCL2L10 and cleaved Caspase 3 protein levels after transfected with pcDNA3.1-BCL2L10 (I) or KD-BCL2L10 (J) for 24 h and then treated with 20 μM cisplatin for another 24 h (I) or 36 h (J) in SKOV3 cells. **(K, L)** Western blot analysis of BCL2L10 protein level after transfected with pZW1-sno-CERNA1 at 0.1, 0.2 μg/mL and pZW1-snoVector (K), or ASO-CERNA1 at 10, 20 nM and ASO-negative control (L), for 24 h in SKOV3 cells. **(M, N)** CCK8 analysis of SKOV3 cell viability. Followed by cisplatin treatment at 20 μM for another 12, 24, 36 and 48 h, pZW1-sno-CERNA1 or pZW1-snoVector plasmid were co-transfected into SKOV3 cells with KD-BCL2L10 or the corresponding negative control for 24 h (M); ASO-CERNA1 or ASO-negative control were co-transfected into SKOV3 cells with pcDNA3.1-BCL2L10 or pcDNA3.1 vector for 24 h (N). **(O,P)** Western blot analysis of cleaved PARP, ATCB and cleaved Caspase 3 protein levels. pZW1-sno-CERNA1 or pZW1-snoVector plasmid were co-transfected into SKOV3 cells with KD-BCL2L10 or the corresponding negative control for 24 h, followed by cisplatin treatment at 20 μM for another 24 h (O); ASO-CERNA1 or ASO-negative control were co-transfected into SKOV3 cells with pcDNA3.1-BCL2L10 or pcDNA3.1 vector for 24 h, followed by cisplatin treatment for another 36 h (P). **(Q, R)** Bisulphite sequencing PCR (BSP) analysis of BCL2L10 promoter DNA methylation level after transfected with pZW1-sno-CERNA1 and pZW1-snoVector at 0.2 μg/mL (Q), or ASO-CERNA1 and ASO-negative control at 20 nM (R), for 24 h in SKOV3 cells. **(S, T)** Chromatin Immunoprecipitation (ChIP) analysis of the binding capacity of DNMT1 with BCL2L10 promoter after transfected with pZW1-sno-CERNA1 and pZW1-snoVector at 0.2 μg/mL (S), or ASO-CERNA1 and ASO-negative control at 20 nM (T), for 24 h in SKOV3 cells. (U) Conceptual schematic of nuclear CERNA1 related regulatory mechanism of OC apoptosis: CERNA1 is transcribed and bind with DNMT1 so as to the moderate DNA methylation level on BCL2L10 promoter under normal conditions. Whereas, in OC, the reduced amount of CERNA1 molecules leads to more DNMT1 binding to BCL2L10 promoter, thereby blocking BCL2L10 expression in OC. Moreover, cisplatin treatment induces the expression of CERNA1. Nuclear CERNA1 decreases the DNA methylation level by decoying DNMT1 from BCL2L10 promoter region and thus induces the expression of BCL2L10 which promotes OC apoptosis. Data are mean ± SEM. of three independent experiments. $^{*}P < 0.05$, $^{**}P < 0.01$ *vs.* control (Ctr). $n \geq 3$.

apoptosis by enhancing BCL2L10 expression, thus reducing the cisplatin resistance.

Considering that BCL2L10 expression might be regulated by the DNA methylation level in its promoter region (Fig. S6A), BSP analysis showed that N-OE-CERNA1 induced the hypomethylation of the BCL2L10 promoter region, while ASO-CERNA1 induced its hypermethylation (Fig. 1Q, R; Fig. S6B). Considering that CERNA1 might bind with DNMT1 and DNMT3B (Table S1), RNA pull-down was performed to determinate the interaction of CERNA1 and DNMT1 (Fig. S6C). An enrichment of CERNA1 in the complex with DNMT1 was further validated by a RIP assay (Fig. S6D, E). Furthermore, a ChIP experiment showed that DNMT1 bound to the BCL2L10 promoter less in cells transfected with the N-OE-CRENA1 plasmid. Conversely, the concomitantly increased binding of DNMT1 to the BCL2L10 promoter was detected after CERNA1 knockdown (Fig. 1S, T). These results suggested that CERNA1 is bound with DNMT1, thereby activating BCL2L10 expression by repressing the interaction between DNMT1 and the BCL2L10 promoter.

In summary, CERNA1 expression was downregulated in OC and was significantly increased in the cisplatin-induced apoptosis. Furthermore, CERNA1 epigenetically activated BCL2L10 expression by decoying DNMT1 from the BCL2L10 promoter, thus enhancing the cisplatin-induced cell apoptosis and overcoming chemoresistance (Fig. 1U).

Conflict of interests

The authors declare no competing interests.

Funding

We appreciated the support from the National Natural Science Foundation of China (No. 81902644), the Natural Science Foundation of Shandong Province (No. ZR2019BC059, ZR2020QH248) and the Key Research and Development Program of Shandong Province, China (No. 2019GSF108126).

Appendix A. Supplementary data

Supplementary data to this article can be found online at https://doi.org/10.1016/j.gendis.2021.12.018.

References

1. Lheureux S, Cristea MC, Bruce JP, et al. Adavosertib plus gemcitabine for platinum-resistant or platinum-refractory recurrent ovarian cancer: a double-blind, randomised, placebo-controlled, phase 2 trial. *Lancet*. 2021;397(10271):281–292.
2. Lheureux S, Gourley C, Vergote I, et al. Epithelial ovarian cancer. *Lancet*. 2019;393(10177):1240–1253.
3. Palazzo AF, Koonin EV. Functional long non-coding RNAs evolve from junk transcripts. *Cell*. 2020;183(5):1151–1161.
4. Calanca N, Abildgaard C, Rainho CA, et al. The interplay between long noncoding RNAs and proteins of the epigenetic machinery in ovarian cancer. *Cancers*. 2020;12(9):2701.
5. Lu W, Huang SY, Su L, et al. Long noncoding RNA LOC100129973 suppresses apoptosis by targeting miR-4707-5p and miR-4767 in vascular endothelial cells. *Sci Rep*. 2016;6:21620.

Rui Xu[a,b,c], Hui Peng[d], Ning Yang[a,e,f], Zhenping Liu[a,e,f], Wei Lu[a,e,f,*]

[a] *Key Laboratory of Gynecologic Oncology of Shandong Province, Department of Obstetrics and Gynecology, Qilu Hospital of Shandong University, Jinan, Shandong 250012, China*
[b] *Department of Clinical Laboratory Medicine, Shandong Provincial Hospital Affiliated to Shandong First Medical University, Jinan, Shandong 250021, China*
[c] *Department of Clinical Laboratory Medicine, Shandong Provincial Hospital Affiliated to Shandong University, Jinan, Shandong 250021, China*
[d] *Department of Obstetrics and Gynecology, The Fifth People's Hospital of Jinan, Jinan, Shandong 250022, China*
[e] *Department of Obstetrics and Gynecology, Qilu Hospital of Shandong University, Jinan, Shandong 250012, China*
[f] *Shandong Engineering Laboratory for Urogynecology, Qilu Hospital of Shandong University, Jinan, Shandong 250012, China*

*Corresponding author. Department of Obstetrics and Gynecology, Qilu Hospital of Shandong University, Jinan, Shandong 250012, China.
E-mail address: luvia@sdu.edu.cn (W. Lu)

1 September 2021
Available online 11 February 2022